Pergamon

Cement and Concrete Research 32 (2002) 1259–1267

CEMENT AND CONCRETE RESEARCH

Characterization of the ASR rim Application to the Potsdam sandstone

Patrice Rivard[a,b,*], Jean-Pierre Ollivier[b], Gérard Ballivy[a]

[a]Centre de Recherche Interuniversitaire sur le Béton (CRIB), Civil Engineering Department, Université de Sherbrooke, Sherbrooke, QC, Canada J1K 2R1
[b]Laboratoire Matériaux et Durabilité des Constructions, INSA-UPS, Toulouse 31077, France

Received 27 March 2001; accepted 19 February 2002

Abstract

Chemical properties of the reaction rim associated with alkali–silica reaction (ASR) were investigated using microprobe and scanning electron microscope (SEM). The studied aggregate is the Potsdam sandstone, a Cambrian siliceous sandstone well known for its reactivity. This particular rock is composed of well-crystallized quartz grains surrounded by a poorly crystallized siliceous cement that is considered to be the reactive constituent. Research was conducted on laboratory concrete specimens having reached various expansion levels and on some samples taken from an ASR-affected dam. Results indicate that the dark rim surrounding reactive particles is mainly composed of silica. This suggests that the reaction rim is formed by the precipitation of dissolved silica. Some alkalis and calcium were detected inside the thin intergranular joints in concentration ranging from 1% to 10%. These ions come from the cement paste and play a major role in dissolving original reactive silica. Crown Copyright © 2002 Published by Elsevier Science Ltd. All rights reserved.

Keywords: Alkali–aggregate reaction; Characterization; Interfacial transition zone; Postdam sandstone

1. Introduction

The Potsdam Cambrian sandstone is responsible for several cases of concrete deterioration due to alkali–silica reaction (ASR) in the Montreal region in Canada [1]. This aggregate is composed of well-crystallized quartz grains surrounded by a poorly crystallized siliceous cement. This cement is considered to be the reactive phase of the rock. One particular petrographic feature associated with ASR is the growth of a dark reaction rim at the periphery of aggregate particles (Fig. 1). The chemical composition of this zone could be different from the inner part of the particle and related to ion exchange processes between silica in aggregates and alkali hydroxides present in concrete pore solution.

A few studies carried out on the reaction rim have been reported in previous papers [2–5]. In each case, the authors conducted their work on opal aggregates and obtained quite similar results. They reported the following trend, from reactive aggregate to cement paste:

- A rapid decrease in SiO_2 content at aggregate contact followed by a slow decrease.
- A rapid increase in CaO content at aggregate contact followed by a slow increase. For instance, Thaulow and Knudsen [2] showed a calcium-rich reaction zone inside the aggregate.
- A maximum alkali content in the middle of the reaction rim, which slowly decreases toward the cement paste.

However, the zone so-called reaction rim, as defined in the studies reported above, is actually a zone surrounding the aggregate, between the particle and the cement paste. In con-crete incorporating Potsdam sandstone, the rim is located at the *internal* periphery of the particles, i.e. within the particle.

2. Scope of work

The study presented in this paper deals with the chemical investigation of the reaction rim surrounding Potsdam

* Corresponding author. Centre de Recherche Interuniversitaire sur le Béton (CRIB), Civil Engineering Department, Université de Sherbrooke, Sherbrooke, QC, Canada J1K 2R1. Tel.: +1-819-821-8000x3916; fax: +1-819-821-7974.
E-mail address: privard@hermes.usherb.ca (P. Rivard).

0008-8846/02/$ – see front matter. Crown Copyright © 2002 Published by Elsevier Science Ltd. All rights reserved.
PII: S0008-8846(02)00765-2

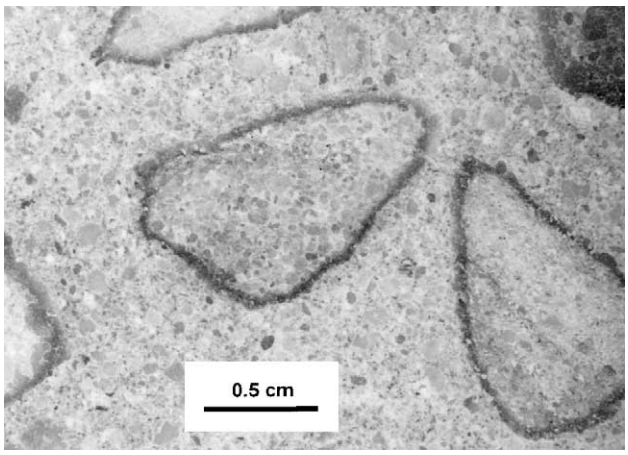

Fig. 1. Reaction rims surrounding Potsdam sandstone particles.

sandstone aggregates in concrete affected by ASR. Microprobe analyses and scanning electron microscope (SEM) analyses were used to characterize variations near to and within the reaction rim.

Two types of concrete incorporating the same aggregate (Potsdam) are investigated in this paper: The first one is a laboratory alkali-boosted mixture kept under accelerated conditions, while the second type consists of a core drilled from a large hydraulic dam exposed to natural conditions. These two sets of samples allow comparison between natural and artificial environmental expositions.

3. Chemical mechanism of ASR

From the classical model proposed by Dent Glasser and Kataoka [6], it is widely accepted that the ASR is initiated by the breaking up of the siloxane bonds by hydroxide ions (OH^-) attack. According to Bulteel et al. [7], this attack creates active sites. This is followed by the dissolution of silica due to the sustained attack by OH^- ions to form mainly $H_2SiO_4^{-2}$ monomers and some small polymers. ASR is initiated where high alkali concentration is found in the cement paste near the reactive particles. Even if alkalis are uniformly distributed in the cement powder, mixing operations lead to variations in the structure and the porosity of the cement paste, and, consequently, to local variations in alkali concentration [8]. Alkali and calcium ions dissolved in pore solution are allowed to migrate through the cement paste and penetrate into aggregate particles. The migration of these cations is possible due to the electric attraction created by the negatively charged particles of silica [9]. The result is a concentration of Ca^{2+}, K^+ and Na^+ within a thin layer surrounding the silica particles [10]. An example of such alkali concentration around aggregate particles has been shown by Rivard et al. [11]. Depending on the concentration of these ions, precipitation products can be formed with dissolved $H_2SiO_4^{-2}$:

$$H_2SiO_4^{-2} + Ca^{2+} \rightarrow CSH$$

$$H_2SiO_4^{-2} + 2K^+ + Na^+ + Ca^{2+} \rightarrow CKSH \text{ (commonly known as ASR silica gel)}$$

Table 1
Chemical composition of Potsdam sandstone

Element	Content (%)
SiO_2	98.7
CO_2	0.42
CaO	0.29
Fe_2O_3	0.23
K_2O	0.15
MgO	0.09
Na_2O	0.08
Al_2O_3	<0.05

4. Materials

A batch of concrete incorporating Potsdam sandstone as coarse aggregate was prepared with a nonreactive fine aggregate derived from granite [12]. The chemical composition of the sandstone is given in Table 1. A normal ASTM Type I high-alkali cement was used. According to the CSA A23.2-14A test procedure, the nominal cement content was 420 kg/m^3 with a water-to-cement ratio of 0.40. NaOH pellets were added to raise the total alkali content of the system to 5.3 kg/m^3, which corresponds to 1.25% Na_2O_{eq}. A set of 12 concrete prisms, 75×75×300 mm, was cast from the concrete mixture. After a curing period of 24 h, test prisms were stored in plastic pails lined with damp terry cloth. The pails were then stored at 38 °C and their length measured periodically. Sample A was kept at 23 °C to hinder the progression of ASR. At selected expansion levels, one prism was removed from the storage condition for analysis. The final expansion level corresponding to each prisms is detailed in Table 2.

A few samples were also collected from a large gravity dam built with Potsdam sandstone. This dam, Beauharnois

Table 2
Expansion level reached by the laboratory samples

Sample	Age (week)	Expansion level (%)
A	2	0
B	13	0.04
C	22	0.06
D	29	0.08
E	36	0.09
F	63	0.14

Table 3
Dectection limits and analytical errors (95% confidence interval)

	Na_2O (%)	K_2O (%)	CaO (%)	SiO_2 (%)
Detection limit	0.12	0.07	0.09	0.11
Mean analytical errors	±0.04	±0.05	±0.33	±0.34

Dam, is located 40 km eastward of Montreal and is suffering from ASR in most of its components [13]. Samples were prepared from a 10 m-long core recovered from the right-wing wall. This part of the dam was constructed in 1929. According to Lupien [14], the overall deformations of the right-wing wall are estimated to vary between 1500 and 2200 microstrains (i.e. 0.15% and 0.22%). The investigated samples exhibited numerous signs of ASR [12]. Moreover, in all of these samples, more than 95% of the aggregate particles showed a reaction rim.

5. Analytical techniques

Three samples were prepared from each concrete prism to be investigated. These samples were submitted to microprobe and SEM analyses. Over 700 spots, mostly located within randomly selected aggregate particles, were analyzed with a Cameca SX50 microprobe at 15 kV and 20 nA. About 20% of the measurements were conducted in cement paste, at regular interval along a straight line originating from aggregate interface. Calibration was done from natural and synthetic control samples. Detection limits and mean analytical errors are presented in Table 3.

Cutting of samples was performed under water, which may have allowed a certain amount of alkalis to be leached out. However, dry polishing was used to limit the loss of alkalis.

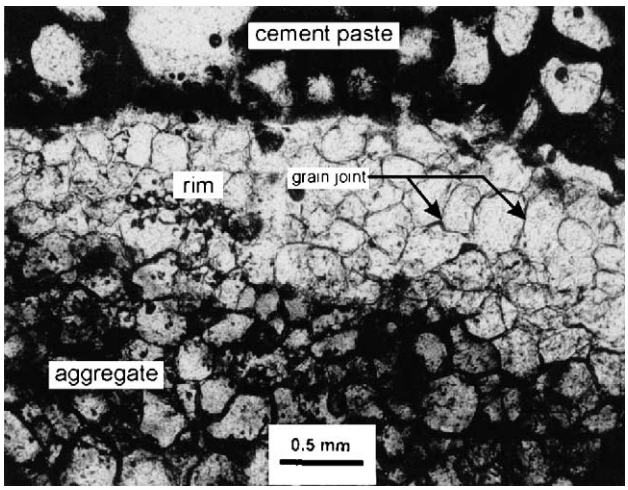

Fig. 2. Reaction rim as seen in thin section; the inner part of the aggregate is extensively deteriorated (dam sample).

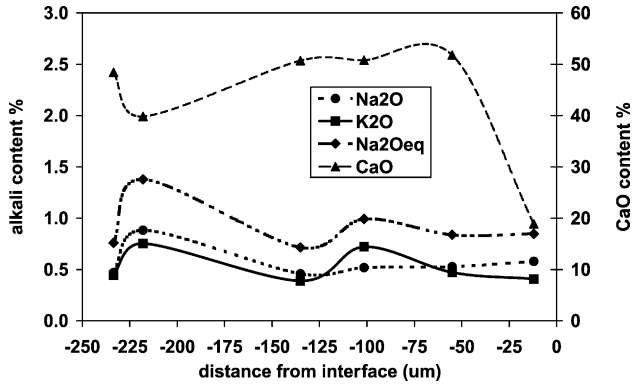

Fig. 3. Profiles of alkalis and CaO in cement paste at expansion level=0%.

6. Results and comments

6.1. Development of the reaction rim

As the reaction progresses and the level of expansion raises, a dark rim is developing at the internal boundary of the aggregate particles. Microprobe analysis revealed that reaction rims are composed of secondary silica surrounding original quartz grain. Fig. 2 shows a rim as seen in thin section prepared from a Beauharnois Dam sample. The inner part of the sandstone particle is severely deteriorated. The reactive intergranular cement is practically dissolved, while quartz grains inside the rim are well cemented. The amount of petrographic features associated with ASR (cracking, silica gel in air void, etc.) also increases with the expansion level of test prisms [12]. No rim can be observed around the particles for the samples analyzed at the beginning of reaction (expansion=0%). At 0.04% expansion, some sandstone particles start to show devel-

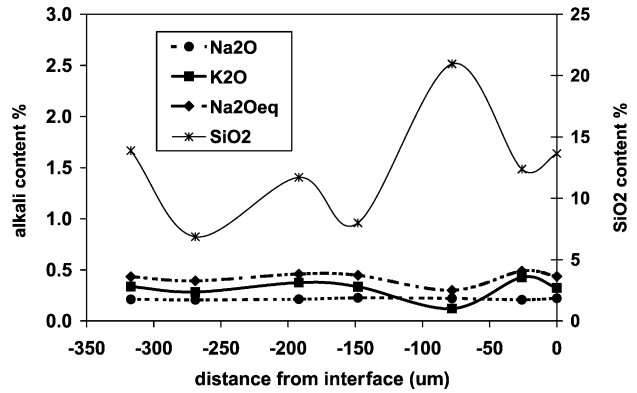

Fig. 4. Profiles of alkalis and SiO_2 in cement paste at expansion level=0.04%.

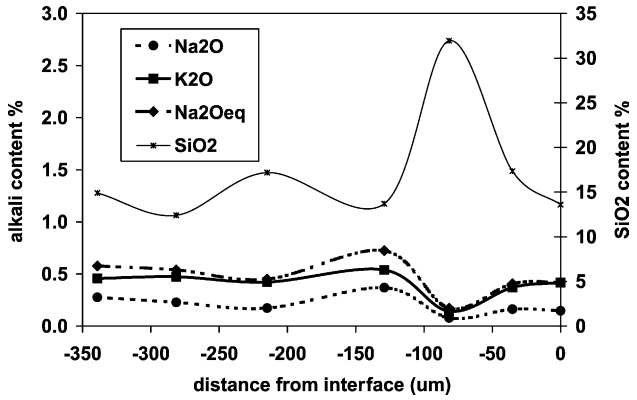

Fig. 5. Profiles of alkalis and SiO_2 in cement paste at expansion level = 0.06%.

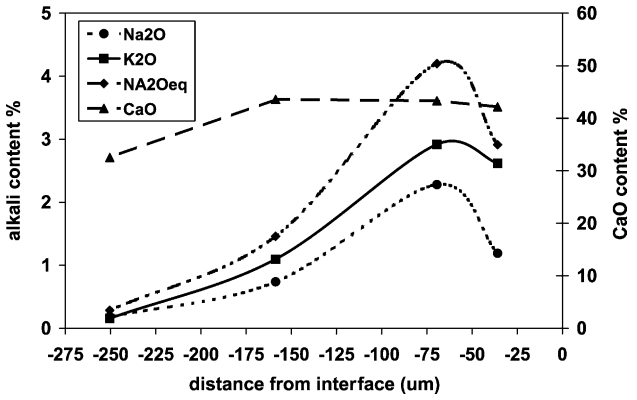

Fig. 7. Profiles of alkalis and CaO in cement paste at expansion level = 0.14%.

oping reaction rims, but rims are generally difficult to identify. At an expansion level of 0.06%, an increasing number of reactive particles show more or less distinct rims, which are about 2 mm thick on average. At 0.12% and 0.14% expansions, reaction rims are much better defined, easily countable and affect nearly all the aggregate particles; dam samples exhibit well-defined rims surrounding more than 95% of the particles.

According to microprobe spot analysis, the chemical composition of the reaction rim is very similar to the global particle. The solid phase consists in pure silica (>99.5%). However, the presence of calcium and alkalis was found inside the thin joints in "secondary" silica surrounding original quartz grains (Fig. 2).

6.2. Microprobe analysis in laboratory samples

6.2.1. Cement paste

Samples prepared from the 14-day specimens indicated more or less homogeneous spreading of alkalis in the cement paste, as measured with microprobe spot analysis (Fig. 3). This was also confirmed by chemical mapping performed on these samples. Assuming that the cement paste porosity is about 30%, microprobe measurements gave a corrected mean value of 1.26% Na_2O_{eq}, which corresponds to the initial theoretical alkali level (1.25%). A mean value of 48% in CaO content was measured, whose distribution also appeared to be uniform, except in the vicinity of aggregate interface where a significant drop was detected (Fig. 3). SiO_2 was also found to be equally spread with a mean value of 10%, but it slightly increases to 14–16% at −50 μm from aggregate interface.

At an expansion level of 0.04%, the distribution of potassium began following a sinusoidal trend. A trough was detected at about −75 μm from the aggregate interface (Fig. 4). The mean value of alkali content in the cement paste decreased. No alkali concentration was found close to aggregate particles and the alkali content was lower compared to the 14-day specimen. A mean value of 12% was found for SiO_2 content, with a peak reaching 21% at −75 μm (Fig. 4).

At an expansion level of 0.06%, the sinusoidal trend has became more defined (Fig. 5). For both expansion levels, calcium was spread homogeneously in the cement paste, with mean values of 46% and 47%. A slight fall was measured near the interface where values dropped to about 39%. SiO_2 mean content in the cement paste raised to 15.1% (Fig. 5). The peak at −75 μm also increased up to 32%.

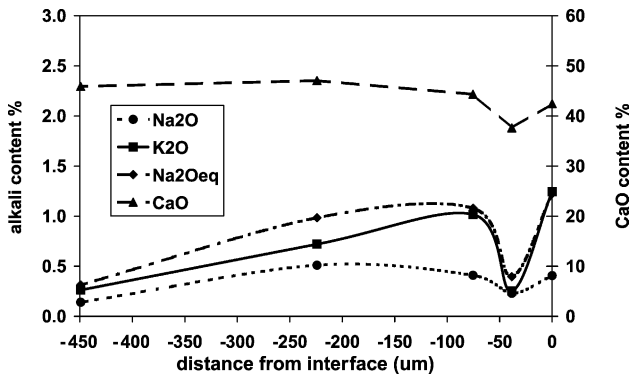

Fig. 6. Profiles of alkalis and CaO in cement paste at expansion level = 0.09%.

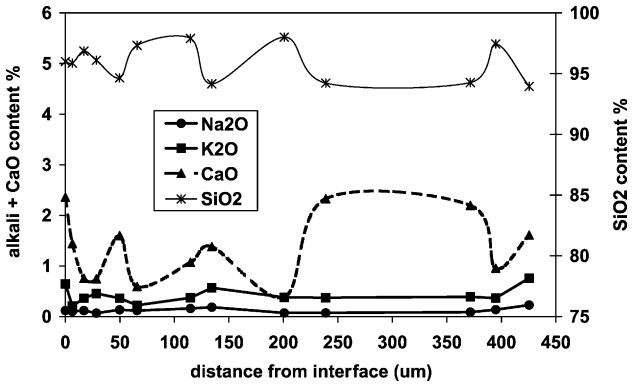

Fig. 8. Profiles of alkalis–CaO and SiO_2 in a grain joint at expansion level = 0%.

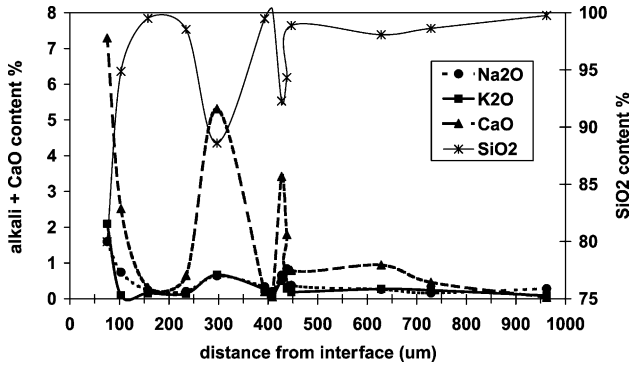

Fig. 9. Profiles of alkalis–CaO in a grain joint at expansion level=0.04%.

Some weeks later, an upward trend in alkali content seemed to occur from the cement paste toward aggregate in 0.09% expansion samples (Fig. 6). However, Na_2O_{eq} maximal values did not exceed the initial value of 1.25%. CaO distribution was quite homogenous with a mean value of 45%, but a trough was detected at −40 μm from the interface (Fig. 6). The SiO_2 peak was found to be closer to the interface at about −40 μm, which corresponds to the CaO trough. SiO_2 mean value remained at 15.1%.

At the highest expansion level (0.14%), only one profile was performed. The rising trend of alkali content was confirmed (Fig. 7). Na_2O_{eq} content culminated at −75 μm with 4.20%. However, a decrease in alkalis was found near the particle interface. CaO content stayed relatively constant. The mean value of SiO_2 content remained at about 15% and no peak was observed. Only four spots were analyzed.

6.2.2. Aggregate particles

The Potsdam sandstone is a porous rock, and about 12% of the aggregate particles showed microcracks before incorporation in concrete [12]. These microcracks stem from tectonics and quarrying operations (i.e. blasting and crushing) and would constitute as many paths for aggressive ions. Therefore, alkali, calcium and hydroxide ions can readily and quickly penetrate particles and move inside. This is confirmed with Sample A, analyzed after 14 days in curing room at 23 °C. Calcium ions started to migrate into aggregate particles through grain joints (Fig. 8). A maximum value of 2.63% in CaO was measured in one profile. A certain sinusoidal trend has emerged. According to our measurements along grain joints, significant amounts of calcium were detected as deep as 425 μm into the particle. However, the alkali concentrations in the grain joints were very low. Maximum values are 0.75% and 0.50% for potassium and sodium, respectively. SiO_2 content varied between 94.0% and 99.4%. Some other measurements showed smoother profiles with lower variations than Fig. 8.

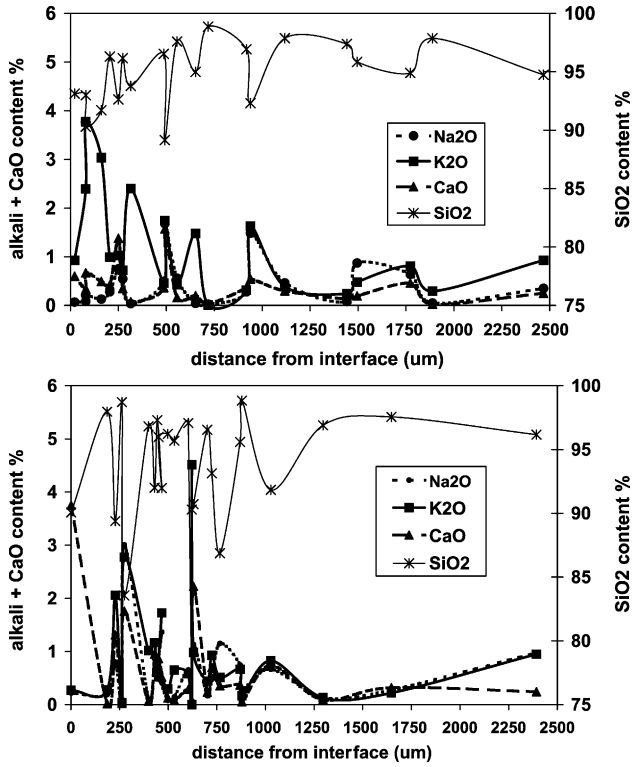

Fig. 11. Profiles of alkalis–CaO and SiO_2 in a grain joint at expansion level=0.08% (two different samples).

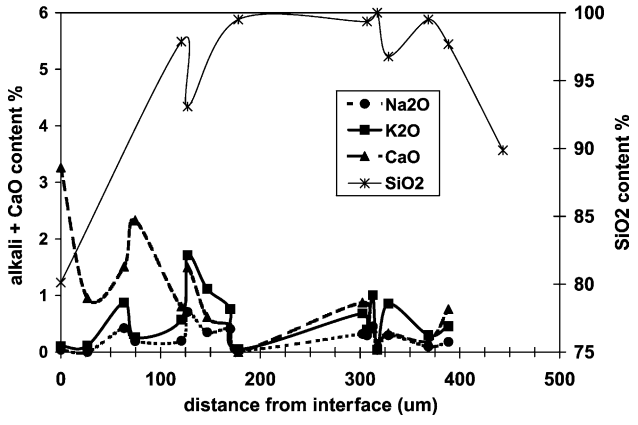

Fig. 10. Profiles of alkalis–CaO and SiO_2 in a grain joint at expansion level=0.06%.

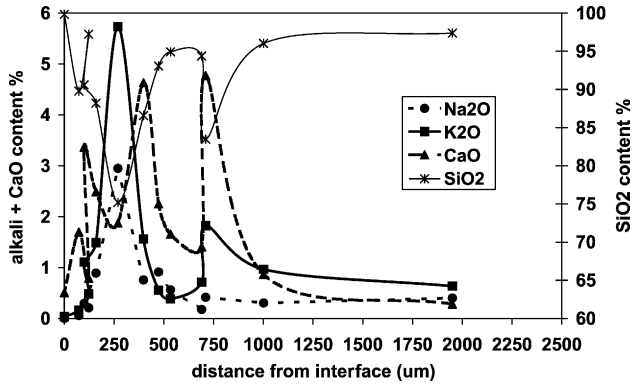

Fig. 12. Profiles of alkalis–CaO and SiO_2 in a grain joint at expansion level=0.09%.

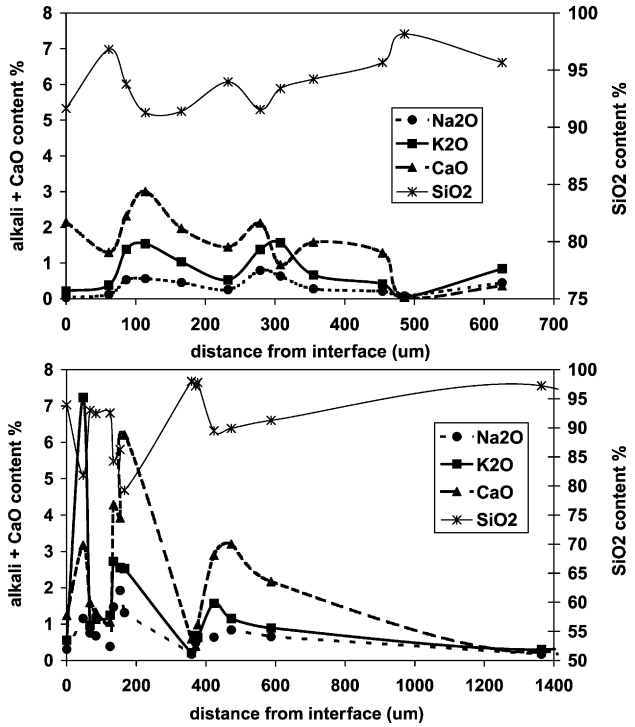

Fig. 13. Profiles of alkalis–CaO and SiO_2 in a grain joint at expansion level=0.14% (two different samples).

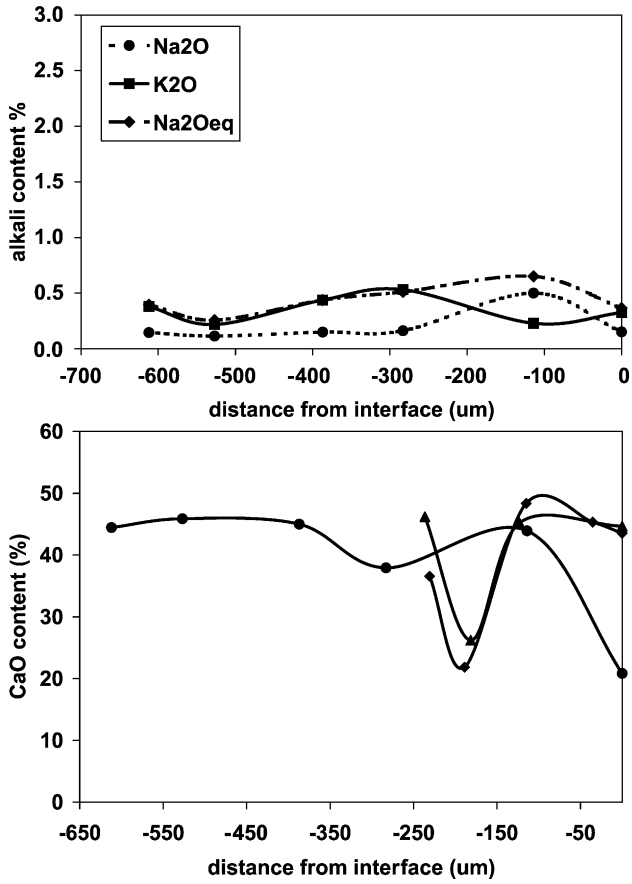

Fig. 14. Profiles of alkalis and CaO in cement paste (same dam sample).

At an expansion level of 0.04%, the CaO content inside grain joint was still high within the first 100 μm from aggregate interface (up to 7.3%). Two other peaks were detected, as seen in Fig. 9. The distribution of alkalis roughly followed the CaO trend, and the sinusoidal profile seemed to be confirmed. The concentration of alkalis remained below 1%. SiO_2 content slightly decreased in the first 200 μm, the lowest value was 94.5%.

Nine weeks later (0.06%), the alkali content began to rise in particles, especially for potassium (Fig. 10). The highest concentrations were found close to the interface, and significant amounts of alkalis and calcium were detected within the first 500 μm. SiO_2 profiles started to show variable contents ranging from 80% to 100%. (Fig. 10b).

A greater dispersion of values was measured at 0.08% expansion (Fig. 11). Higher amounts of potassium and sodium were found inside aggregate particles. A particular succession of peaks and troughs was also observed. The dissolution of silica can be seen in Fig. 11 where lower amounts were measured close to the aggregate interface.

At expansion level of 0.09%, profiles were variable, but the sinusoidal trend was again observed (Fig. 12). Maximal values were CaO=4.77%, K_2O=5.74% and Na_2O=2.95%. The trend observed on the 0.08% samples was kept. High SiO_2 values were measured at about 100 μm (97–99%), followed by a succession of peaks and troughs until 1000 μm where SiO_2 tended to become constant at ±97% (Fig. 12).

At the highest expansion level (0.14%), the profiles were similar to those observed on previous samples (Fig. 13). In most cases, weak concentrations were found within the first 25 μm. Significant amounts of alkalis and calcium were measured at least 700 μm inside particles. Peaks and troughs were located at various distances from aggregate interface. Maximum values were measured in the same sample (CaO=6.20%, K_2O=7.24%, Na_2O=2.00%). Regarding SiO_2 content, profiles were variable (Fig. 13). A minimum

Table 4
Chemical measurements of dam samples

	Na_2O (%)		K_2O (%)		Na_2O_{eq} (%)		CaO (%)		SiO_2 (%)	
Location	Minimum	Maximum	Minimum	Maximum	Minimum	Maximum	Minimum	Maximum	Minimum	Maximum
Cement paste adjacent to aggregate	0.02	0.64	0.02	0.53	0.02	0.72	21.1	48.2	4.71	58.1
Reaction rim	0.01	0.50	0.03	1.81	0.05	1.50	0.00	5.28	91.5	99.3

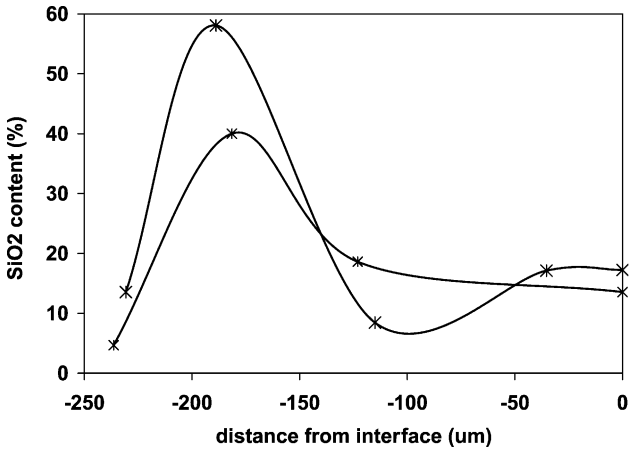

Fig. 15. Profiles of SiO_2 in cement paste (two different dam samples).

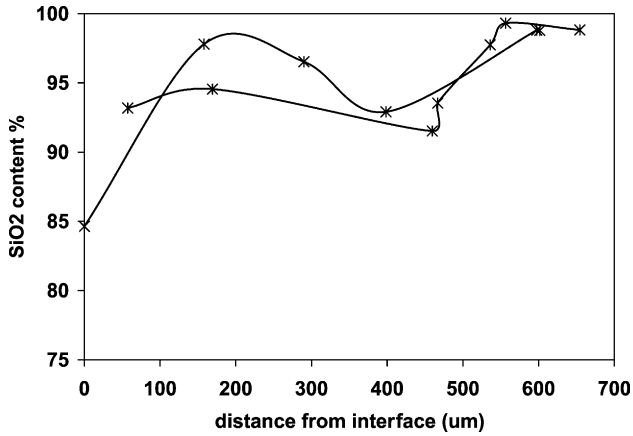

Fig. 17. Profile of SiO_2 in a grain joint (two different dam samples).

value of 79% was measured. Troughs in SiO_2 content corresponded to alkali peaks.

6.3. Microprobe analysis in dam samples

6.3.1. Cement paste

Spot analyses were performed on three samples prepared from the Beauharnois Dam core. Table 4 provides the minimum and maximum values measured with microprobe.

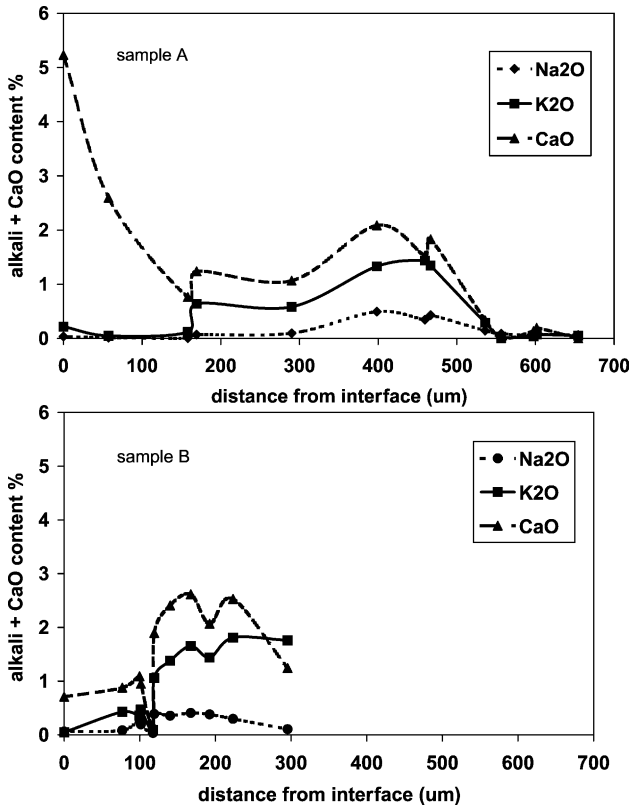

Fig. 16. Profile of alkalis and CaO in a grain joint (two different dam samples).

A certain distribution of the alkalis was observed in the cement paste, even though microprobe measurements were very low (Na_2O_{eq}<0.8%). As in laboratory specimens, potassium was more abundant than sodium and both elements followed a similar trend. On every profiles performed in the dam sample, a peak was reached at about 100–125 μm from the aggregate interface. However, in one case, the potassium peak was out of phase compared to sodium (Fig. 14a). Calcium content showed a different trend. The mean value was about 45%, but two troughs were found at about 200 μm away from the interface. (Fig. 14b). In one case, a drop was measured at the aggregate interface, but the distribution appeared to be uniform in the rest of the cement paste. SiO_2 content in the cement paste showed the same trend in each samples analyzed during this study. A mean value of about 17% was measured close to particle with a clear peak at about −175 μm (Fig. 15).

6.3.2. Aggregate particles

The reaction rim is well developed and easily visible. SEM observations showed that the rim was severely cracked at a few places, likely due to the swelling pressures created by the gel inside the particle.

In one case, high calcium content was measured in joint grain near the particle interface (Fig. 16). Concentrations in calcium and potassium quickly increased at about 125–150 μm inside the particle, while sodium concentration did not vary much, remaining below 0.5%. According to the measurements performed on one sample, the alkali and calcium content drastically decreased at a distance of 550 μm and did not subsequently reach values above 0.2%. SO_2 content was relatively high and did not show much variation (Fig. 17).

7. Discussion

The development of the rim is associated with the progressive disintegration of sandstone particles. Besides,

some studies report that, in concrete immersed in NaOH solution, sandstone particles become so friable that quartz grains can be removed by nail rubbing. Two observations must be highlighted: (1) During the ongoing process of ASR, the intergranular siliceous cement, the reactive phase, is attacked and dissolved by hydroxides. (2) A rim cementing quartz grains develops as the content of alkalis and calcium within this rim increases. These phenomena suggest that intense physico-chemical activities occur at the paste–aggregate interface. Actually, the rim corresponds to a densification of the aggregate boundary (Fig. 18). Rims should not be considered impermeable because reactions are still going on after their formation.

Based on the results previously detailed, the following mechanism can be proposed. Hydroxide, calcium, potassium and sodium ions dissolved in the pore solution quickly move inward sandstone particles by taking the preferential paths, which are microcracks and connected porosity. The intergranular silica is dissolved by hydroxides, as silica tends to migrate outward. The reaction first occurs at the aggregate–cement paste interface. However, due to the relatively high permeability of the rock particle, the reaction quickly processes deeper. From our results, calcium seems to penetrate faster than alkalis. This is in contradiction with some other papers, which stated that calcium ions tend to stay at the surface of particles. With the presence of alkalis and calcium, some silica can form silica gel within the particle as observed with SEM. Some other dissolved silica precipitates close the aggregate–cement paste interface, forming the reaction rim. In the cement paste, some silica also seem to move outside. In our laboratory samples, peaks in silica are observed in the first 100 μm from aggregate interface. This peak is located at 175 μm in the Beauharnois Dam samples. A previous study [12] reported that, in concrete having reached high expansion levels, Potsdam sandstone particles seemed to have underwent a "global" swelling. Unlike other aggregate types, silica gel is mainly found within aggregate particles, which would allow isotropic expansion pressures.

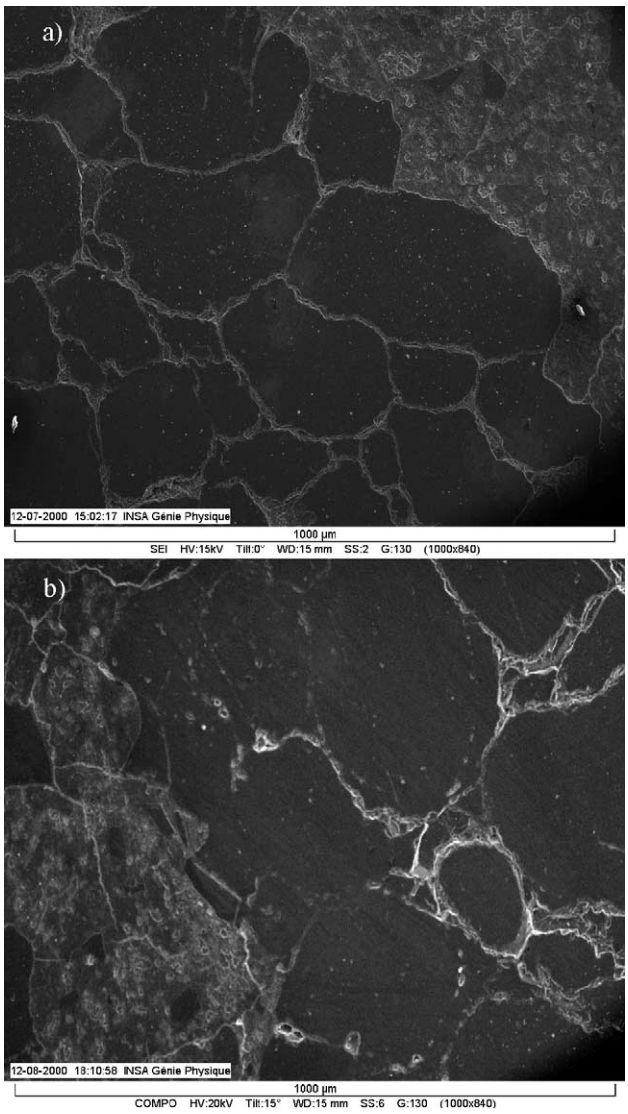

Fig. 18. Deterioration of the aggregate particle and densification of the reaction rim: (a) expansion = 0%; (b) expansion = 0.09%.

Data obtained from measurements inside aggregates can be considered as reliable. The summation of all elements detected by microprobe at each measurement spot was most of the time close to 100%, with a mean value of 98.1% and a standard deviation of 1.6. Variations in alkali and silica content would then be directly related to ions migration and to the dissolution of silica. On the other hand, the summation of all elements falls to 67.7% (standard deviation = 6.7) for measurements performed in the cement paste. This is mainly due to the fact that the porosity of the paste is much higher and variable than aggregates porosity. Values were not corrected with respect to this information, i.e. normalized to 100%. A certain part of the fluctuations in cement paste data can be ascribed to the heterogeneous porosity of the paste.

Another fact that must be taken into account is the possible leaching of some alkalis during the sample preparation steps (cutting). A certain amount of alkalis might have been leached out leading to an underestimation of the alkali content in reaction rims. Moreover, microprobe high current has probably caused some evaporation of alkalis.

Microprobe analysis did not provide an explanation of the colour difference between the rim and the rest of the particle.

8. Conclusion

Most of the studies previously published have been carried out on opal aggregates. Thus, ASR process in these cases can be schematized as a sphere of pure reactive silica attacked by hydroxide ions. However, not all rocks react like opal: The Potsdam sandstone is an excellent example.

The reaction rim is mainly composed of pure silica (>99.5%). Nevertheless, the alkali and calcium contents

measured into thin joints between quartz grains increase as the reaction progresses, while silica content tends to decrease. Calcium is the most abundant cation, followed by potassium and sodium, respectively. The reaction may be schematized as follows:

1. quick penetration of calcium, alkali and hydroxide ions into aggregate particles through microcracks and connected porosity;
2. dissolution of the reactive silica cementing quartz grains;
3. precipitation of some silica within the particle at the interface with the cement paste;
4. growing of the reaction rim and densification of the aggregate interface;
5. formation of silica gel inside aggregates, leading to global swelling of particles; and
6. aggressive ion penetration into particle cracks in reaction rims and migration through grain joints.

The dark colour of the rim could not be clearly explained. All these remarks are based on data obtained through the present investigation on the Potsdam sandstone. A different aggregate type, such as an opal or a limestone, would not react like this particular sandstone does. More work is needed to gain better understanding of deterioration mechanisms and formation of reaction rim regarding this particular aggregate.

Acknowledgments

The authors would like to thank Philippe de Parseval and Nathalie Ruscassier for their help regarding the microprobe and the SEM, as well as Carole Causserand for the chemical analysis of the sandstone. The contributions of Éric Dessureault and Geneviève Petit are also acknowledged. Work at the LMDC of Toulouse (France) has been realized with the financial support of the Fond pour la Formation de Chercheurs et l'Aide à la Recherche du Quebec (FCAR). We thank Hydro-Quebec for providing the dam core. This research project is supported by the Natural Sciences and Engineering Council of Canada (NSERC).

References

[1] J. Bérard, N. Lapierre, Réactivités aux alcalis du grès de Potsdam dans les bétons, Can. J. Civ. Eng. 4 (3) (1977) 332–344.
[2] N. Thaulow, T. Knudsen, Quantitative microanalysis of the reaction zone between cement paste and opal, Proceedings of the Symposium on AAR, Preventive Measures, Reykjavik (Iceland), August, ACI local chapter, Montreal, 1975, pp. 189–203.
[3] A.B. Poole, Proceedings of the 3rd International Symposium on the Effect of Alkalis on the Properties of Concrete, Copenhagen (Denmark), ACI local chapter, Montreal, 1976, pp. 163–176.
[4] H. Wang, J.E. Gillot, Mechanism of alkali–silica reaction and the significance of calcium hydroxide, Cem. Concr. Res. 21 (1991) 647–654.
[5] M. Brouxel, The alkali–aggregate reaction rim: Na_2O, SiO_2, K_2O, and CaO chemical distribution, Cem. Concr. Res. 23 (1993) 309–320.
[6] L.S. Dent Glasser, N. Kataoka, The chemistry of alkali–aggregate reaction, Proceedings of the 5th International Conference on AAR, Cape Town (South Africa), National Research Building Institute, Pretoria, 1981 (Paper S252/23), 7 p.
[7] D. Bulteel, E. Garcia-Diaz, J.M. Siwak, C. Vernet, H. Zanni, Alkali–aggregate reaction: A method to quantify the reaction degree, Proceedings of the 11th International Conference on AAR, Quebec City (Canada), CRIB, Quebec City, 2000, pp. 11–20.
[8] A.B. Poole, C.F. Mole, K.N. Shrapel, Alkali–silica reaction in concrete related to alkali diffusion through the cement pore network, Proceedings of the 11th International Conference on AAR, Quebec City (Canada), CRIB, Quebec City, 2000, pp. 209–218.
[9] G.H. Bolt, Determination of the charge density of silica sols, J. Phys. Chem. 61 (9) (1957) 1166–1169.
[10] S. Chatterji, N. Thaulow, Some fundamental aspects of alkali–silica reaction, Proceedings of the 11th International Conference on AAR, Quebec City (Canada), CRIB, Quebec City, 2000, pp. 21–29.
[11] P. Rivard, G. Ballivy, B. Fournier, Evaluation of the interfacial transition zone in concrete affected by alkali–silica reaction, Proceedings of the 2nd International RILEM Conference on the ITZ in Cementitious Composites, Haifa (Israel), E&FN Spon, London, 1998, pp. 114–121.
[12] P. Rivard, B. Fournier, G. Ballivy, Quantitative petrographic technique for concrete damage due to ASR: Experimental and application, Cem., Concr., Aggregates 22 (1) (2000) 63–72.
[13] V. Gocevski, Réfection des ouvrages hydroélectriques affectés par la réaction alcalis–granulat (expérience de la centrale Beauharnois), Proceedings of the Annual Progress in Concrete Seminar, Eastern Ontario and Quebec Chapter of ACI, Montréal (Canada), 1998, 13 p.
[14] R. Lupien, Gonflement du béton de Beauharnois, Comité de révision de la sécurité des barrages, Hydro-Québec, report crsb-d.doc, 1995.